Draft version April 1, 2021
Typeset using LaTeX **preprint2** style in AASTeX63

ULTRA-FAINT DWARF GALAXIES: SHEDDING LIGHT ON DARK MATTER

Hannah Richstein[1] and Nitya Kallivayalil[1]

[1] *University of Virginia*
530 McCormick Road
Charlottesville, VA 22904, USA

ABSTRACT

Ultra-faint dwarf (UFD) galaxies are among the oldest, least chemically-enriched, most dark matter dominated stellar populations discovered to date. Using deep *Hubble Space Telescope* ACS/WFC observations, we perform aperture photometry to generate source catalogs. To characterize the UFDs in terms of age and metallicity, we use distance-minimalization to fit Victoria-Regina isochrones. Specifically, we look at the co-added populations of 27 UFDs, as well as the separate co-added populations of two groups of UFDs, five that are considered long-term Milky Way (MW) satellites and three associated with the Large Magellanic Cloud (LMC). The "characteristic" UFD is best fit by an isochrone with age 13.6 Gyr and [Fe/H]=-2.0. The long-term MW satellites are fit by a 13.2 Gyr, [Fe/H]=-1.8 isochrone, while the LMC-associated UFDs are fit with an 11.5 Gyr, [Fe/H]=-1.2 isochrone. These results offer tantalizing evidence for how the environment around UFDs may have affected their star-formation histories.

Keywords: ultra-faint dwarf galaxies; near-field cosmology

1. INTRODUCTION

The age of large sky surveys such as SDSS, PAN-STARRS, and DES, among many others (York et al. 2000; Chambers et al. 2016; Abbott et al. 2018), has pushed the limits of our observational technologies and more than doubled the number of known Milky Way (MW) satellites (e.g., Koposov et al. 2015; Laevens et al. 2015), with the current population being $\sim$ 60. About half of these satellites fall into the category of ultra-faint, with stellar masses ($M_{*}<10^5 M_{\odot}$). Ultra-faint dwarf satellites (UFDs) distinguish themselves from "classical" or "bright" dwarf galaxies by their absolute luminosities of less than 10^5 solar luminosity, and from satellite star clusters based on adherence to a luminosity-metallicity relationship, high stellar velocity dispersions (indicating high mass-to-light ratios, given how few stars they have), low metallicities, and evidence of extended episodes of star formation (Simon 2019).

1.1. Λ *Cold Dark Matter*

UFDs are highly dark matter dominated, with mass-to-light ratios sometimes on the order of 1000. Such dark matter dominated systems may serve as the best laboratories for probing the nature of dark matter and whether Lambda Cold Dark Matter (ΛCDM; the most widely accepted cosmological model) is supported on small scales. Traditionally, ΛCDM has been excellent for characterizing what we observe on large scales, but does not perform as well on scales smaller than 1 Mpc; this makes such regimes particularly intriguing for further investigating existing tensions (e.g., Bullock & Boylan-Kolchin 2017).

1.2. *"Satellites of Satellites"*

The ΛCDM model presents adiabatic fluctuations as the primordial seed which led to the cosmic structure we observe today. Due to inflation and gravitational instability, these fluctuations grew to be over-dense regions and eventually collapsed into dark matter halos. These halos, in turn, should have their own substructure, according to N-body simulations (e.g., Bullock & Boylan-Kolchin 2017). Halos that correspond to a Milky-Way-type galaxy should then be found to have substructure, however what we observe around our Galaxy does not seem to support this. By looking more closely at our Local Group neighbors, we can observe these discrepancies on a highly-resolved level.

Opposite UFDs, the two largest MW satellites, the Large and Small Magellanic Clouds (LMC and SMC, respectively), have been visible with the naked eye from the Southern Hemisphere for millennia. ΛCDM predicts that dark matter has a self-similar nature, which suggests that in the same way the Magellanic Clouds are satellites of the Milky Way, they, too, have their own satellite galaxies. Recent works such as Kallivayalil et al. (2018) have used *Gaia* DR2 (Gaia Collaboration et al. 2018) to confirm this, showing likely associations between at least four of these ultra-faint satellites and the LMC.

These "satellites of satellites" are particularly interesting to study in relation to ΛCDM as simulations suggest that low-mass dark matter halos form early and are pulled into smaller hosts before they can be absorbed into larger ones (Navarro et al. 1997). Thus, the UFD satellites of the LMC may have been able to continue forming stars for longer than those that fell directly into the MW (Diemand et al. 2008; Wheeler et al. 2015). By analyzing the stellar populations of LMC satellites versus long-term MW satellites, we can determine whether there is observational support for this part of ΛCDM.

The LMC-associated satellites analyzed in this study are Horologium 1, Phoenix 2, and Reticulum 2, while the long-term MW satellites are Hydra 2, Pegasus 3, Sagittarius 2, Triangulum 2, and Tucana 2. These groups were assigned based on Patel et al. (2020), which took the known proper motions of the UFDs and calculated orbital histories while taking into account the potentials of the MW, LMC, and SMC. We chose long-term MW satellites specifically because they are the most likely to have already been in the MW halo during the epoch of reionization (e.g., Zaroubi 2013). Comparing the stellar populations of LMC-associated satellites with those of long-term MW satellites could yield information about how the effects of reionization differed based on environment.

1.3. *Satellite Planes*

Another issue with ΛCDM on small scales is that satellites around both the Milky Way and M31 seem to lie on a plane around their respective galaxies, inconsistent with predictions that these satellites should be distributed either spherically, isotropically, or in a prolate ellipsoid around their host galaxy. This growing issue is also supported by the 3D-motions of the satellites, which suggest a preferred orbital pole that is normal to the apparent plane of satellites (Bullock & Boylan-Kolchin 2017).

To determine whether this "plane of satellites" is a real structure and not just a coincidental juxtaposition of satellites, the bulk proper motions of each satellite must be known. To calculate proper motions, there need to be at least two observations taken over a long enough baseline that the stars were able to noticeably move. As this Treasury program only includes first-epoch imaging, follow-up observations using HST or the *James Webb Space Telescope* (JWST) will be necessary in the coming years.

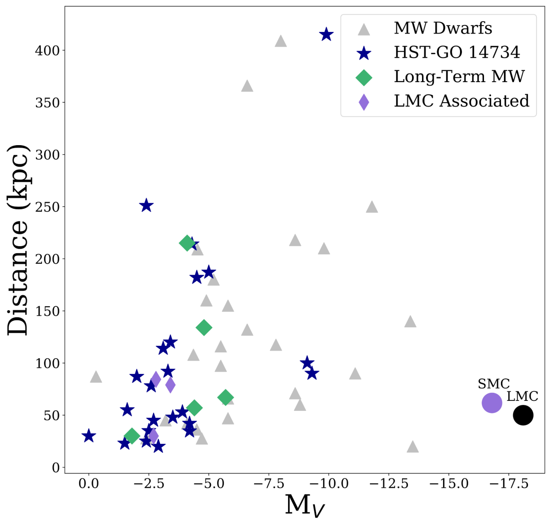

Figure 1. Distance of MW satellite galaxies as a function of absolute magnitude (gray triangles); long-term MW candidates (green square diamonds); "satellites of satellites" candidates (purple skinny diamonds); other satellites in the Treasury program (navy stars). The LMC (SMC) is marked as a black (purple) circle.

Target	**Dist. Modulus**	**LMC or MW**
Horologium 1	19.60	LMC
Hydra 2	20.89	MW
Pegasus 3	21.70	MW
Phoenix 2	19.52	LMC
Reticulum 2	17.50	LMC
Sagittarius 2	19.10	MW
Triangulum 2	17.27	MW
Tucana 2	18.80	MW

Table 1. Target names of the eight UFD satellites analyzed in this study. Distance moduli from Fritz et al. (2018) and association with LMC or MW from Patel et al. (2020).

1.4. *The Characteristic UFD*

As the entire UFD population is among our more recently discovered Galactic neighbors, with the first one being discovered in 2005 (Willman et al.) using data from the Sloan Digital Sky Survey (SDSS) (York et al. 2000), the Treasury program has provided the largest uniformly-observed sample to-date. Because of this, they are able to be considered not just as singular entities, but also as a group, without having to worry about the effects of using data sets from many different telescopes. Here, we will briefly examine how the combined stellar populations of the Treasury UFDs can be described.

2. DATA AND PHOTOMETRY

2.1. *Observations*

The observations were taken using the F606W and F814W filters of the *Hubble Space Telescope* (HST) ACS/WFC (Treasury Program 14734; PI: Kallivayalil). The 30 targets of the program were chosen because they lacked sufficient ACS/WFC imaging and either because follow-up HST/JWST imaging would obtain better bulk proper motions (PMs) for them than *Gaia* or because HST/JWST would provide the only avenue to measure internal motions. The UFD targets are shown in Figure 1 as blue stars (unknown association), green square diamonds (long-term MW), and purple skinny diamonds (LMC-associated). Other MW dwarf galaxies are plotted as grey triangles, while the LMC and SMC are black and purple circles, respectively.

The basic observing strategy included four dithered 1100s exposures in both F606W and F814W for each target. Eight of the thirty targets were chosen for deeper analysis in this paper either because they have been found to have either a likely association with the LMC or because they are believed to be long-term Milky Way satellites (Kallivayalil et al. 2018; Erkal & Belokurov 2020; Patel et al. 2020). Of the satellites included in this study, listed in Table 1, Tucana II and Triangulum II required two pointings each to ensure that we would not be star limited, due to intrinsic faintness and extension, respectively.

2.2. *Reduction and Creation of Source Catalogs*

Source catalogs were created for 27 of the 30 original targets for this analysis, with Phoenix I and Carina excluded because they are considered to be "classical" dwarfs, and Reticulum 3 because the separate observations were not properly aligned. The images were processed through the current ACS pipeline, which corrected for charge-transfer inefficiency (CTI), and the separate dithers were combined using the DRIZZLE package (Fruchter & Hook 2002) to create the drc files.

The `photutils` (Bradley et al. 2020) routines `DAOStarFinder` and `aperture_photometry` were used to detect sources and to calculate the flux inside circular apertures of four-pixel radii, which was then converted to STMAG. The drc files were also run through `SExtractor` (Bertin & Arnouts 1996) for source detection using a three-pixel radius in order to obtain the `class_star` diagnostic, which assigns values based on the likelihood of the source being a star or not (increasing likelihood from 0 to 1). The F606W and F814W lists were matched, yielding a list of only the sources present in both filters.

The CTI-corrected separate dither images, or flc files, were run though the same `photutils` routines as the drc files. Sources were matched across the four separate dithers in each filter using a 6D linear transformation. The sigma-clipped median magnitude value of each source was taken and compared to the single `photutils` drc magnitude to account for instrumental zeropoint effects. The overall median offset between the source lists was added to the flc magnitudes. The source magnitudes were extinction-corrected using the Schlafly & Finkbeiner (2011) recalibration of the Schlegel et al. (1998) dust maps.

To move into absolute magnitude space, the distance moduli listed in Table 1 were subtracted from the final apparent magnitude values. To derive an empirical error for the sources, we took the sigma-clipped, standard deviation of the flc magnitudes for each matching source in the two filters. For the analysis, only sources with `class_star` values greater than or equal to 0.95 in both filters were used.

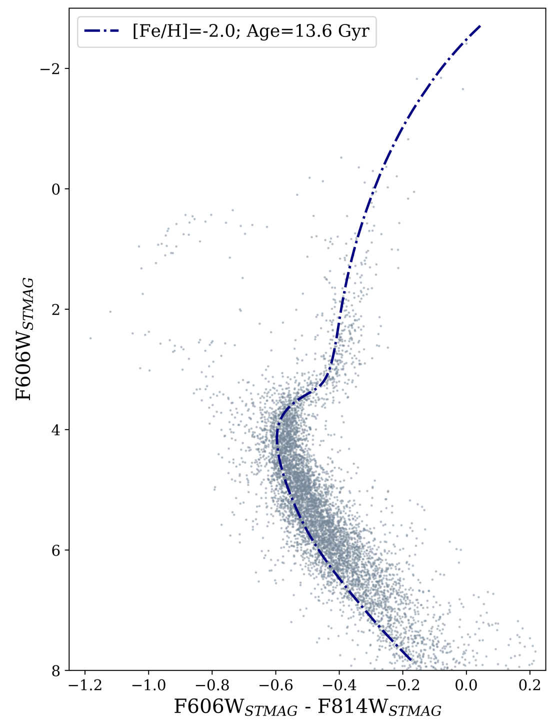

Figure 2. The sources (dark grey points) from 27 Treasury UFD targets overlaid in absolute magnitude space. The best-fitting Victoria-Regina isochrone according to the distance-minimization method ([Fe/H]=-2.0; Age=13.6 Gyr) is overplotted in navy blue.

3. ANALYSIS

To characterize the UFD population as a whole, we co-added the 27 target stellar populations in absolute magnitude space, resulting in a "stacked" color-magnitude diagram (CMD). We then iterated through a catalog Victoria-Regina isochrones (VandenBerg et al. 2006) with ages between 10.5 and 13.8 Gyr and [Fe/H] values between −2.8 and −1.2. To fit the isochrone, we calculated the minimum distances from each source to each of the isochrone points between

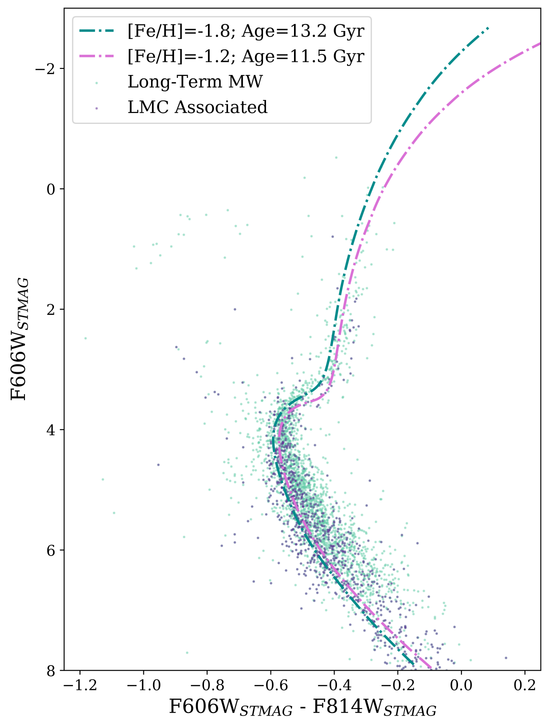

Figure 3. The sources from the long-term MW and LMC associated UFDs, in light green and purple, respectively. Their best-fitting isochrones are overplotted in green and orchid dashed lines.

the absolute F606W magnitude values of 2 and 4, which bracket the main sequence turnoff (MSTO). The best-fitting isochrone using this method corresponds to an age of 13.6 Gyr and an [Fe/H] value of -2.0. It is shown overlaid on the "stacked" CMD in Figure 2.

We used the same method to fit isochrones to the co-added long-term MW UFDs and the LMC-associated stellar populations. Figure 3 shows the long-term MW sources in green, while the LMC-associated sources are in purple. The best-fitting isochrones are 13.2 Gyr with an [Fe/H]=-1.8 for the MW UFDs and 11.5 Gyr with an [Fe/H]=-1.2 for the LMC-associated satellites. These are overplotted in green and orchid, respectively.

4. CONCLUSIONS

As expected, the best-fitting isochrone for the combined UFD stellar populations described them as very old and metal-poor. The same can be said for the stellar populations of the two groups of UFDs, although the specific ages and [Fe/H] values are noticeably different. The long-term MW satellites have an estimated age of 13.2 Gyr, which is older than that of the LMC-associated satellites by 1.7 Gyr. The MW UFDs are also more metal-poor, by 0.6 dex. Taken together, these two parameters support the idea that the LMC satellites could have had a longer star-formation period than the MW UFDs. The more metal-rich fit could be explained by the stellar populations having more time to evolve - with more supernovae occurring to enrich the gas reservoirs that would be used for new generations of star formation.

To confirm these isochrone fits, it is necessary to derive detailed star-formation histories (SFHs). A forthcoming paper (Sacchi et al., in prep) using the photometry catalogs described here includes these SFHs and shows how the cumulative star-formation histories of the long-term MW and LMC-associated satellites differ and compares them with respect to the epoch of reionization.

This work has introduced the HST Treasury sample of UFDs and has shown how uniform observations of such a large number of targets can be combined to draw insights that might otherwise have been riddled with systematics. We have found tantalizing evidence of a significant difference between the populations of two subgroups of UFDs that further analysis will help underscore. While we wait for a second-epoch of observations, there is still much more to be learned from the data we have in hand.

We will be examining the morphology of individual UFDs and comparing their surface brightness profiles to those of simulated galaxies, as well as using the available orbital information to determine how their distances relative to the MW may have factored in to events in their SFHs. By learning all that we can about UFDs and how they interact with their environments, we will make progress in our understanding of ΛCDM on small scales and the seemingly elusive nature of dark matter.

ACKNOWLEDGEMENTS

HR would like to thank Paul Zivick, Mattia Libralato, Elena Sacchi, and Jack Warfield for useful conversations regarding the photometry process. Support for this work was provided by NASA through grants for program GO-14734 from the Space Telescope Science Institute (STScI), which is operated by the Association of Universities for Research Astronomy (AURA), Inc., under NASA contract NASS-26555. This research has made use of NASA's Astrophysics Data System.

Facility: HST

Software: photutils (Bradley et al. 2020), SExtractor (Bertin & Arnouts 1996)

REFERENCES

Abbott, T. M. C., Abdalla, F. B., Allam, S., et al. 2018, ApJS, 239, 18. doi:10.3847/1538-4365/aae9f0

Bertin, E. & Arnouts, S. 1996, A&AS, 117, 393. doi:10.1051/aas:1996164

Bradley, L., Sipocz, B., Robitaille, T., et al. 2020, Zenodo. doi:10.5281/zenodo.4044744

Bullock, J. S., & Boylan-Kolchin, M. 2017, ARA&A, 55, 343

Chambers, K. C., Magnier, E. A., Metcalfe, N., et al. 2016, arXiv:1612.05560

Diemand, J., Kuhlen, M., Madau, P., et al. 2008, Nature, 454, 735. doi:10.1038/nature07153

Erkal, D. & Belokurov, V. A. 2020, MNRAS, 495, 2554. doi:10.1093/mnras/staa1238

Fritz, T. K., Battaglia, G., Pawlowski, M. S., et al. 2018, A&A, 619, A103. doi:10.1051/0004-6361/201833343

Fruchter, A. S. & Hook, R. N. 2002, PASP, 114, 144. doi:10.1086/338393

Gaia Collaboration, Brown, A. G. A., Vallenari, A., et al. 2018, A&A, 616, A1. doi:10.1051/0004-6361/201833051

Kallivayalil, N., Sales, L. V., Zivick, P., et al. 2018, ApJ, 867, 19. doi:10.3847/1538-4357/aadfee

Koposov, S. E., Belokurov, V., Torrealba, G., et al. 2015, ApJ, 805, 130

Laevens, B. P. M., Martin, N. F., Bernard, E. J., et al. 2015, ApJ, 813, 44

Navarro, J. F., Frenk, C. S., & White, S. D. M. 1997, ApJ, 490, 493. doi:10.1086/304888

Navarro, J. F., Ludlow, A., Springel, V., et al. 2010, MNRAS, 402, 21

Patel, E., Kallivayalil, N., Garavito-Camargo, N., et al. 2020, ApJ, 893, 121. doi:10.3847/1538-4357/ab7b75

Schlafly, E. F. & Finkbeiner, D. P. 2011, ApJ, 737, 103. doi:10.1088/0004-637X/737/2/103

Schlegel, D. J., Finkbeiner, D. P., & Davis, M. 1998, ApJ, 500, 525. doi:10.1086/305772

Simon, J. D. 2019, ARA&A, 57, 375

VandenBerg, D. A., Bergbusch, P. A., & Dowler, P. D. 2006, ApJS, 162, 375. doi:10.1086/498451

Wheeler, C., Oñorbe, J., Bullock, J. S., et al. 2015, MNRAS, 453, 1305. doi:10.1093/mnras/stv1691

Willman, B., Blanton, M. R., West, A. A., et al. 2005, AJ, 129, 2692

York, D. G., Adelman, J., Anderson, J. E., et al. 2000, AJ, 120, 1579. doi:10.1086/301513

Zaroubi, S. 2013, The First Galaxies, 45. doi:10.1007/978-3-642-32362-1_2